Nuclear Science and Techniques **23** (2012) 237–241

A 16-channel gated integrator for high-resolution energy spectroscopy systems

ZHOU Chaoyang[1,2] SU Hong[1] KONG Jie[1] DONG Chengfu[1] QIAN Yi[1] YANG Haibo[1,2] MA Xiaoli[1]

[1] *Institute of Modern Physics, Chinese Academy of Sciences, Lanzhou 730000, China*

[2] *Graduate University of Chinese Academy of Sciences, Beijing 100049, China*

Abstract A 16-channel gated integrator (GI) module following semi-Gaussian shaping amplifiers was developed for high-resolution energy spectroscopy systems at Institute of Modern Physics, Chinese Academy of Sciences. This GI solved the ballistic deficit problem by integrating the signal until all the charge was collected from the detector at counting rates up to 100 K. In this paper, a fast shaper was used to optimize the gate logic to ensure nonlinearity of the GI less than 0.17%; and a novel compensation approach, to reduce the charge injection from the switches in the GI; and a T-switch configuration, to eliminate leakage current in the reset switch.

Key words Energy spectroscopy, Gated integrator, Charge injection compensation, Leakage current elimination.

1 Introduction

With the development of radioactive ion beam physics at Institute of Modern Physics, Chinese Academy of Sciences, high-resolution energy spectroscopy systems were employed in many experiments[1], with different detector arrays of HPGe Clover detectors, silicon strip detectors and large area scintillators. We developed a 16-channel gated integrator (GI), of single-width NIM module, with a bank of semi-Gaussian shaping amplifiers, for different detectors to acquire energy information in those systems. Compared with peak detecting ADCs in traditional energy spectroscopy systems for pulse amplitude analysis, a GI amplifier automatically eliminates the ballistic deficit effect caused by changes in charge collection time of the detectors. This of significance in the energy resolution and dead time at the short shaping time constants required for ultra-high counting rates[2].

GI amplifier modules have been implemented in ORTEC Model 673 and 973, and products by other manufactures, where a single channel of signal processing circuit is used for high-resolution energy spectroscopy[3]. For our system combining multiple circuits with a multi-channel data acquisition (DAQ) system based on PCI eX tensions for instrumentation (PXI) hardware, the GI is used as a multiple channel module. We are able to meet the channel-by-channel requirements with such a dense implementation[4], enabling this 16-channel GI module to function nicely with a number of detector families.

In this paper, the structure and timing of the 16-channel GI module are described. The relationship between the amplitude of Gaussian shaped input and the maximum of GI output is analyzed. Techniques of fast shaping, charge injection compensation and leak current elimination in the design, are described, too.

2 GI in an energy spectroscopy system

Figure 1 is a block diagram of a spectroscopy system with a 16-channel GI. The detector signals are amplified and pre-shaped by preamplifiers and semi-Gaussian shaping amplifiers. The wide bandwidth output from the shaping amplifier is fed into a fast

Supported by the Important Direction Project of the CAS Knowledge Innovation Program (No.KJCX2-YW-N27) and the National Natural Science Foundation of China (No.11005135).

* Corresponding author. *E-mail address*: suhong@impcas.ac.cn

Received date: 2012-02-28

shaper to generate a trigger which forms the gate logic of the GI. The semi-Gaussian output is integrated on the feedback capacitor (C_F). Then the peak value of GI output is acquired by a PXI based DAQ system. The timing diagrams of the trigger and readout logic are presented in Fig.2.

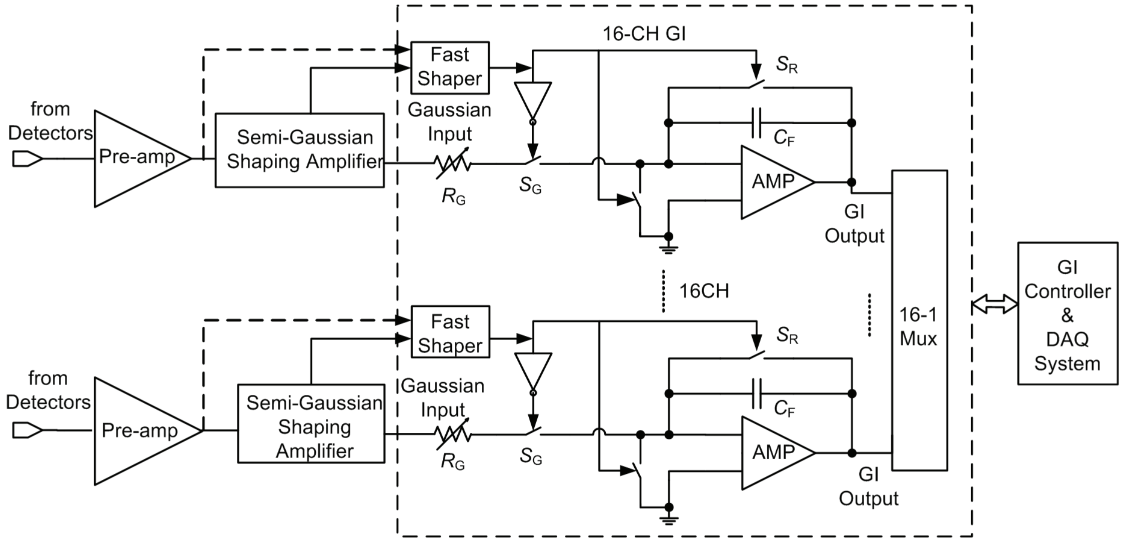

Fig.1 Block diagram of an energy spectroscopy system with a 16-channel GI.

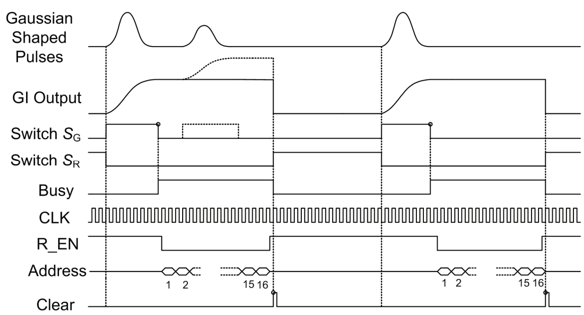

Fig.2 Time diagrams for accepted events. The pulse edge marked with a circle is the source of others at this moment.

Before the Gaussian shaped pulse arrives, switch S_G is open while switch S_R is closed, causing the gated-integrator output to be at ground potential. At the instant, the Gaussian shaped pulse arrives, a trigger signal is generated. Switch S_G closes and S_R opens, and the semi-Gaussian signal is integrated on capacitor C_F as described in Eq.(1).

$$V_{GI} = \frac{1}{C_F R_G} \int_0^T V_{GA} \mathrm{d}t + V_0 \quad (1)$$

where, V_{GA} and V_{GI} are the output of the Gaussian shaping amplifier and *a* GI channel, respectively.

The integration period is set to last as long as the longest semi-Gaussian pulse duration. After the integration, switch S_G is off, and the output of the GI is held. Meanwhile, a busy signal is generated to avoid new triggers during the event processing, which is to minimize the spectral distortion caused by two or more ions arriving at the detector within one amplifier pulse width. When all the 16 channels are in a “hold” state, a read-enable signal is sent to ADC card. According to the address offered by the GI controller, the outputs of the 16 channels are serially acquired by a 16-1 multiplexer. The reset and busy signal are held until a shot-duration clear signal arrives, witch is generated at the end of the acquisition process. The dead time of the system consists of two parts: one is the duration of the semi-Gaussian signal generation and the other is the acquisition time for the 16 channels. For this real time system, the counting rates can be up to 100 kHz.

It was reported that ballistic deficit affected systems with HPGe Clover detectors and large area scintillators, which vary significantly in their charge collection[5,6]. In this paper, for detectors having little ballistic deficit effects, like silicon strip detectors, the linear relationship between the Gaussian pulse height and the GI output is analyzed. A GI amplifier integrates the Gaussian waveform for its full duration. Its peak amplitude equals the area under the unipolar curve. According to the integral formula of Gaussian function, the amplitude of Gaussian input signal A_{GA} is proportional to the maximum of GI output A_{GI}.

$$A_{GI}R_GC_F=KA_{GA}\tau \quad (2)$$

where, K is the scale factor, and τ is the shaping time of the semi-Gaussian shaping amplifier. Certain values for R_G and C_F can keep A_{GI} and A_{GA} in good linearity for different semi-Gaussian shaping amplifiers.

3 The circuit design

The circuit is implemented in a single-width NIM module. Fig.3 shows the side view of the 16-channel GI module. Every channel is in a separate narrow board, which is installed on the base board.

Techniques used in this circuit, such as fast shaping, charge injection compensation and leakage current reduction, will be introduced in this section.

Fig.3 Side view of the 16-channel GI module with cover removed.

3.1 Fast shaper

To integrate the whole area under the Gaussian waveform, a trigger was needed as early as possible for generating control logic to the switches in the GI. A fast shaper followed by a discriminator was introduced to offer a trigger which came after the Gaussian shaped pulse within less than 30 ns.

Figure 4 shows the structure of a fast shaper. It consists of a differential stage, a gain stage and an integral stage. Either the preamplifier output which contains high-frequency component or the Gaussian signal which is slower can be shaped with a small rise time by this fast shaper. For a Gaussian input, a large value of the capacitor in the differential stage is chosen, and the rise time of the Gaussian signal will be decreased from a few microseconds to several hundred nanoseconds. For systems using a fast signal, only the differential stage of the fast shaper will be used, and a small value of the capacitor is chosen in order to make the rise time of the fast shaper output at a few tens of nanoseconds.

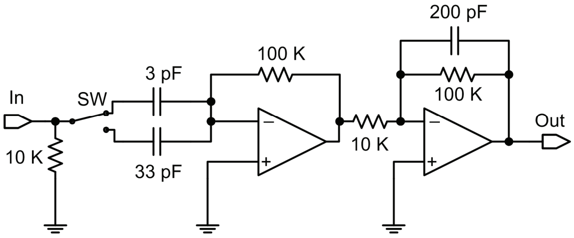

Fig. 4 The fast shaper with three stages.

3.2 Charge injection compensation

DMOS switches SD5400 were chosen as switches in the GI. When a transient voltage excursion appeared at the gate, there would be an injection of electric charge into analog path via the gate-to-drain and the gate-to-source capacitances, which would cause errors to the GI output. The network indicated by the dotted line in Fig.5 was used to compensate this charge injection.

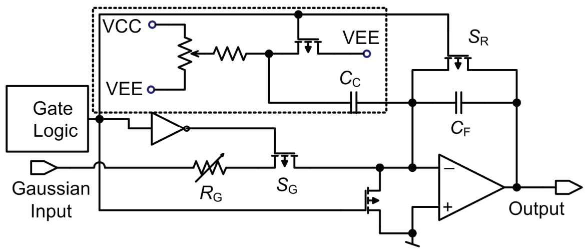

Fig.5 Schematics of the GI with a network for charge injection compensation.

When the state of switches is changed, certain quantity of charge will be injected into the inverting input via the capacitor C_C by the compensation network. This is opposite to the charge injected by switches. Since it is known that the amount of charge injected is equal to the product of the voltage excursion amplitude on the component and its capacitance, generating a product equal magnitude but opposite polarity can be used to compensate for this effect. After analysis and experimental trials, C_C was chosen to be 10 pF. Thus by changing the amplitude of the voltage excursion on C_C, the error of the output voltage caused by charge injection was reduced to less than 2 mV.

3.3 T-switch configuration to prevent leak current

While the GI is in "integration" or "hold" state, the reset switch has to be kept off. However the effect of leakage current in the GI reset switch will cause errors to the output in the long duration of these states. To eliminate this effect, the single reset switch was replaced by the T-switch configuration in Fig.6.

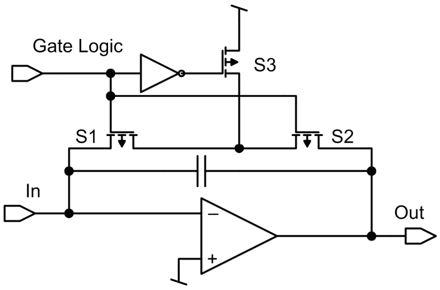

Fig.6 A T-switch configuration as the reset switch.

The leakage current of the DMOS switch is composed of the source/body reverse leakage current and the drain/source sub-threshold current. Since the source/body reverse leakage current can be negligible in SD5400, the drain to source sub-threshold current becomes the main factor of the "off" current. If the source and body are at the same potential, the drain/source current of a MOS transistor in the deep sub-threshold region of operation is given by

$$I_{\rm DS} \approx I_{\rm DO}\frac{W}{L}{\rm e}^{V_{\rm GS}/nV_{\rm T}}(1-{\rm e}^{V_{\rm DS}/V_{\rm T}}) \quad (3)$$

where, $I_{\rm DS}$ is the drain to source current of the transistor, $I_{\rm DO}$ is the saturation current, $V_{\rm GS}$ is the gate to source voltage, $V_{\rm DS}$ is the drain to source voltage, W/L is the ratio of width to length of the transistor, and $V_{\rm T}$ is the threshold voltage of the transistor. Eq.(3) shows, even for $V_{\rm GS}$=0, the only way to establish a zero switch leakage current is to set $V_{\rm DS}$ to 0 V. To maintain the $V_{\rm DS}$ of the DMOS switch at virtual ground, a T-switch configuration shown in Fig. 6 was used to replace the single reset switch. The T-switch configuration was composed of two DMOS switches, *S*1, *S*2, in series and a grounded DMOS switch, *S*3, attached to the node between the two switches. When the two DMOS switches in parallel with the integration capacitor are off, the third switch, *S*3, is on. Thus, in this configuration, $V_{\rm DS}$ of the switch connected to the inverting input of the GI is maintained at 0 V, and very little leakage current flows through this switch.

4 Measurements

A complete set of measurements was performed in the lab in order to characterize performances of the GI module. Fig.7 shows the waveform of the GI when the spectroscopy amplifier model 572 from ORTEC was selected to supply the input signal. The linearity for one channel of the GI is shown in Fig.8. In this example the amplitude of pulses fed into ORTEC 572 was the independent variable.

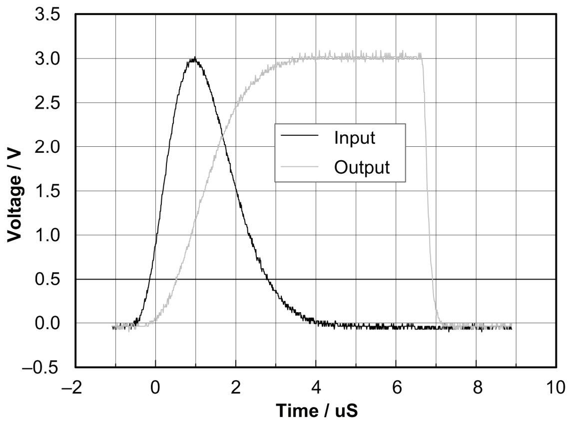

Fig.7 Output waveform of the GI to a Gaussian shaped input.

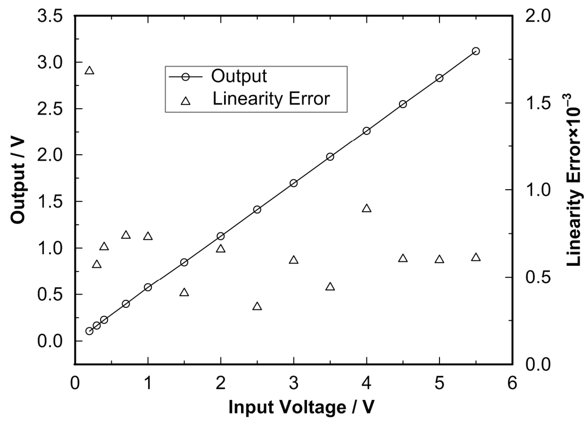

Fig.8 Linearity of the GI for one channel.

Specifications of the GI are given in Table 1, which is the worst all over the 16 channels. Every channel was also calibrated. Fig.9 shows the outputs of all the 16 channels when the amplitude of pulses fed into ORTEC 572 is 0.6 V and 0.8 V. Additionally, the long-term stability was evaluated after the 16-channel GI module worked for 60 h. The output differences for 0.6 V input are shown in Fig.10.

Table 1 Specifications of the GI.

Parameters	Value
Full scale output / V	±6V
Linearity error / %	<0.17
Voltage output noise (rms) / mV	<2.2
Droop rate / $mV \cdot mS^{-1}$	<0.5
Counting rate / k	<100

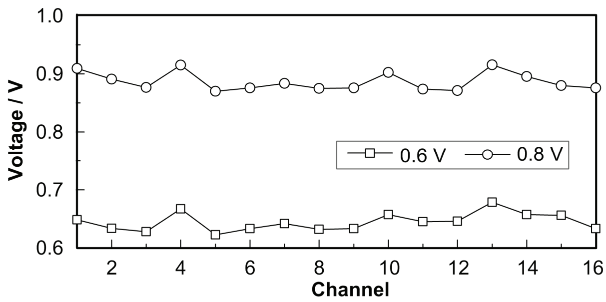

Fig.9 Outputs of all the 16 channels of the GI.

5 Conclusions

A 16-channel GI had been developed and tested. The high degree of linearity was achieved by using novel techniques. This high event rate capability insured that the circuit would perform well in high-resolution energy spectroscopy systems.

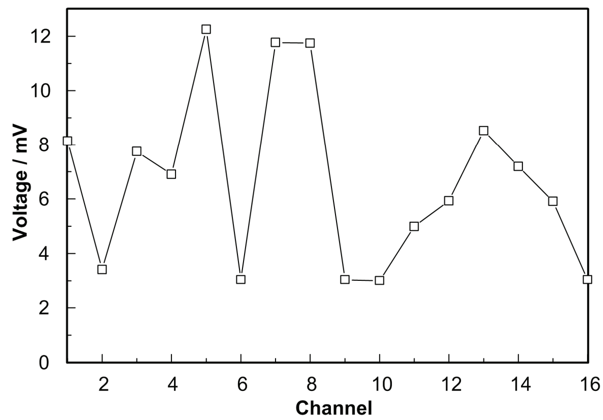

Fig.10 Output differences of the 16 channels for 60 h.

References

1 Sun Z, Zhan W L, Guo Z Y, *et al.* Nucl Instrum Meth A, 2003, **503:** 496–503.

2 Becker T H, Gross E E, Trammell R C, Trans Nucl Sci, 1981, **NS28:** 598–602.

3 Pauly S W, Nucl Instrum Meth A. 1999, **422:** 379–384.

4 Kong J, Su H, Chen Z H, *et al.* Nucl Instrum Meth A, 2010, **622:** 215–218.

5 Britton C L, Becker T H, Paulus T J, *et al.* Trans Nucl Sci, 1984, **NS-31:** 455–460.

6 Gal J, Hegyesi G, Kalink G, *et al.* Nucl Instrum Meth A, 1997, **399:** 407–413.